Phase transition of the Ising model on a fractal lattice

Jozef Genzor,[1] Andrej Gendiar,[1,*] and Tomotoshi Nishino[2]
[1]*Institute of Physics, Slovak Academy of Sciences, Dúbravská cesta 9, SK-845 11 Bratislava, Slovakia*
[2]*Department of Physics, Graduate School of Science, Kobe University, Kobe 657-8501, Japan*
(Received 18 September 2015; published 22 January 2016)

The phase transition of the Ising model is investigated on a planar lattice that has a fractal structure. On the lattice, the number of bonds that cross the border of a finite area is doubled when the linear size of the area is extended by a factor of 4. The free energy and the spontaneous magnetization of the system are obtained by means of the higher-order tensor renormalization group method. The system exhibits the order-disorder phase transition, where the critical indices are different from those of the square-lattice Ising model. An exponential decay is observed in the density-matrix spectrum even at the critical point. It is possible to interpret that the system is less entangled because of the fractal geometry.

DOI: 10.1103/PhysRevE.93.012141

I. INTRODUCTION

Phase transitions and critical phenomena have been some of the central issues in statistical analyses of condensed matter physics [1]. When a second-order phase transition is observed, thermodynamic functions, such as the free energy, the internal energy, and the magnetization, show nontrivial behavior around the transition temperature T_c [2,3]. This critical singularity reflects the absence of any scale length at T_c, and the power-law behavior of thermodynamic functions around the transition is explained by the concept of the renormalization group [1,4–6].

Analytic investigations of the renormalization group flow in a φ^4 model show that the Ising model exhibits a phase transition when the lattice dimension is larger than one, which is the lower critical dimension [6,7]. In a certain sense, the one-dimensional Ising model shows rescaled critical phenomena around $T_c = 0$. When the lattice dimension is larger than four, which is the upper critical dimension, and provided that the system is uniform, then the Ising model on regular lattices exhibits mean-field-like critical behavior.

Compared with critical phenomena on regular lattices, much less is known about fractal lattices. Renormalization flow has been investigated by Gefen *et al.* [8–11], where correspondence between the lattice structure and the value of critical indices is not fully understood in a quantitative manner. For example, the Ising model on a Sierpinski gasket does not exhibit a phase transition at any finite temperature, although the Hausdorff dimension of the lattice, $d_H = \ln 3/\ln 2 \approx 1.585$, is larger than one [12,13]. The absence of a phase transition could be explained by the fact that the number of interfaces, i.e., the outgoing bonds from a finite area, does not increase when the size of the area is doubled on the gasket. A nontrivial feature of this system is that there is a logarithmic scaling behavior in the internal energy toward zero temperature [14]. The effect of anisotropy has been considered recently [15]. In case of an Ising model on a Sierpinski carpet, the presence of a phase transition is proved [16], and its critical indices were roughly estimated by Monte Carlo simulations [17]. It should be noted that it is not easy to collect a sufficient number of data plots for finite-size scaling [18] on such fractal lattices by means of Monte Carlo simulations, because of the exponential blowup of the number of sites in a unit of a fractal.

In this article, we investigate the Ising model on a planar fractal lattice, shown in Fig. 1. The lattice consists of vertices around the lattice points, which are denoted by the open dots in the figure, where there are Ising spins. The whole lattice is constructed by recursive extension processes, where the linear size of the system increases by a factor of 4 in each step. If the lattice was a regular square one, $4 \times 4 = 16$ units are connected in the extension process, whereas only 12 units are connected on this fractal lattice; four units are missing in the corners. As a result, the number of sites contained in a cluster after n extensions is $N_n = 12^n$, and the Hausdorff dimension of this lattice is $d_H = \ln 12/\ln 4 \approx 1.792$. The number of outgoing bonds from a cluster is only doubled in each extension process since the sites and the bonds at each corner are missing. If we evaluate the lattice dimension from the relation

$$M = L^{d-1} \tag{1}$$

between the linear dimension L and the number of outgoing bonds M, we have $d = 1.5$, since M is proportional to $\sqrt{L}$ on the fractal. We remark that the value is different from $d_H \approx 1.792$.

We report the critical behavior of the Ising model on the fractal lattice when the system size is large enough. The thermodynamic properties of the system have been numerically studied by means of the higher-order tensor renormalization group (HOTRG) method [19]. The system exhibits an order-disorder phase transition, where the critical indices are different from the square-lattice Ising model. In the next section we will introduce a representation of the Ising model in terms of a vertex model, which is suitable for numerical analyses by means of the HOTRG method. In Sec. III, we show the calculated result around the transition temperature T_c. Conclusions are summarized in the last section.

II. VERTEX REPRESENTATION

We introduce a representation of the Ising model as a (symmetric) 16-vertex model. The Ising interaction between two adjacent Ising spins σ and σ', where each one takes either

*andrej.gendiar@savba.sk

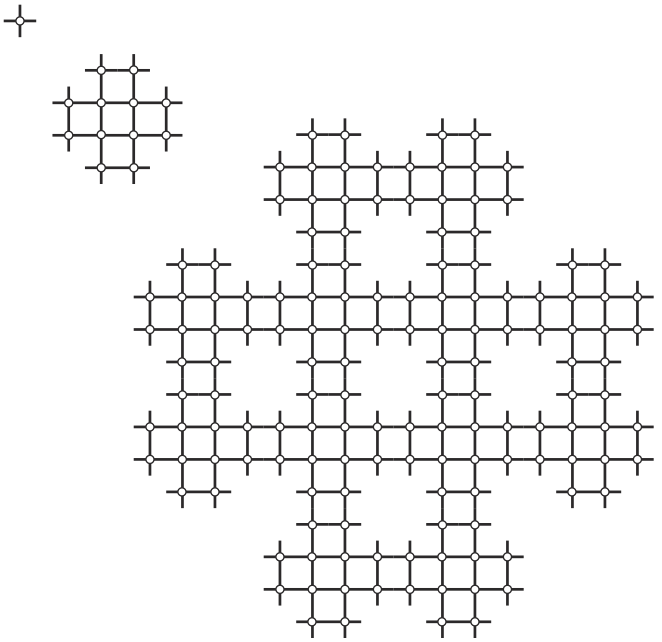

FIG. 1. Composition of the fractal lattice. Upper left: A local vertex around an Ising spin shown by the open dot. Middle: The basic cluster which contains $N_1 = 12$ vertices. Lower right: The extended cluster which contains $N_2 = 12^2$ vertices. In each step of the system extension, the linear size of the system increases by a factor of 4, where only 12 units are linked, and where four units at the corners are missing, if it is compared with a 4×4 square cluster.

$+1$ or -1, is represented by the diagonal Hamiltonian

$$H(\sigma,\sigma') = -J\sigma\sigma', \tag{2}$$

where $J > 0$ represents the ferromagnetic coupling. Throughout this article we assume that there is no external magnetic field. The corresponding local Boltzmann weight on the bond is given by

$$\exp\left[-\frac{H(\sigma,\sigma')}{k_{\rm B}T}\right] = \exp\left[\frac{J}{k_{\rm B}T}\sigma\sigma'\right] = e^{K\sigma\sigma'}, \tag{3}$$

where T is the temperature, $k_{\rm B}$ is the Boltzmann constant, and we have introduced a parameter $K = J/k_{\rm B}T$.

It is possible to factorize the bond weight $e^{K\sigma\sigma'}$ into two parts, by introducing an auxiliary spin $s = \pm 1$, which is often called an "ancilla," and which is located between σ and σ' [20]. A key relation is

$$e^{K\sigma\sigma'} = \frac{1}{2(\cosh 2\overline{K})^{1/2}} \sum_s e^{\overline{K}s(\sigma+\sigma')}, \tag{4}$$

where the right-hand side (rhs) takes the value $(\cosh 2\overline{K})^{1/2}$ when $\sigma = \sigma'$, and $(\cosh 2\overline{K})^{-1/2}$ when $\sigma \neq \sigma'$, and where Eq. (4) holds under the condition

$$e^{K} = (\cosh 2\overline{K})^{1/2}. \tag{5}$$

The new parameter $\overline{K}$ is then expressed as follows,

$$e^{\overline{K}} = \sqrt{e^{2K} + \sqrt{e^{4K} - 1}}. \tag{6}$$

Thus, if we introduce a factor

$$W_{\sigma s} = e^{\overline{K}\sigma s}[2(\cosh 2\overline{K})^{1/2}]^{-1/2} \tag{7}$$

for each division of a bond, we can rewrite the Ising interaction in the following form,

$$e^{K\sigma\sigma'} = \sum_s W_{\sigma s} W_{\sigma' s}. \tag{8}$$

By means of the factorization in Eq. (8), we can map the square-lattice Ising model into a symmetric 16-vertex model, where the local vertex weight is defined as

$$T_{s\,s's''s'''} = \sum_\sigma W_{\sigma s} W_{\sigma s'} W_{\sigma s''} W_{\sigma s'''}. \tag{9}$$

In the upper-left-hand corner of Fig. 1, we have shown the graphical representation of the vertex weight $T_{s\,s's''s'''}$, where the open circle denotes the Ising spin σ, which is summed up. The four short bars around the Ising spin in Fig. 1 show the halves of the bonds, where there are auxiliary spins s, s', s'', and s''' at the end of each short bar.

In case we consider a finite-size cluster with a rectangular shape with free boundary conditions, we have to prepare a new boundary Boltzmann weight,

$$P_{s\,s's''} = \sum_\sigma W_{\sigma s} W_{\sigma s'} W_{\sigma s''}, \tag{10}$$

and a corner Boltzmann weight,

$$C_{s\,s'} = \sum_\sigma W_{\sigma s} W_{\sigma s'}. \tag{11}$$

It should be noted that these boundary weights $P_{s\,s's''}$ and $C_{s\,s'}$ are obtained by taking a partial trace for the vertex weight; we have the relations

$$P_{s\,s's''} = \frac{\sum_{s'''} T_{s\,s's''s'''}}{\sum_{s'''} W_{\sigma s'''}} \tag{12}$$

and

$$C_{s\,s'} = \frac{\sum_{s''s'''} T_{s\,s's''s'''}}{\left(\sum_{s''} W_{\sigma s''}\right)\left(\sum_{s'''} W_{\sigma s'''}\right)}, \tag{13}$$

where one can neglect the denominator when one is interested in the critical singularity; the denominators just subtract a regular function from the free energy of the system. In case one needs fixed boundary conditions, it is sufficient to avoid taking the configuration sum for σ in the rhs of both Eqs. (10) and (11), and to set all the boundary spins to be either $+1$ or -1 according to the condition. The vertex weights $T_{s\,s's''s'''}$, $P_{s\,s's''}$, and $C_{s\,s'}$ are invariant under arbitrary permutation of the indices.

There are various choices of the factorization of the bond weight in Eq. (8). Instead of using the relation in Eq. (7), one can introduce an asymmetric decomposition

$$W = \begin{pmatrix} \sqrt{\cosh K}, & \sqrt{\sinh K} \\ \sqrt{\cosh K}, & -\sqrt{\sinh K} \end{pmatrix}, \tag{14}$$

where we have used the matrix notation for the weight $W_{\sigma s}$. This expression is often employed in the tensor network formulations [19], which does not require any typical symmetry for

local weights, as long as the numerical treatment is concerned. In case this asymmetric factorization in Eq. (14) is employed, one has to care about the order of the indices in $T_{s\,s's''s'''}$ [21]. In the following numerical calculation, we use a symmetric factorization.

The fractal lattice we treat in this article is constructed by a recursive joining process of the local tensors, which is nothing but a vertex weight in Eq. (9) at the beginning. In each extension process, we join 12 local tensors, as shown in the middle of Fig. 1. In the joining process, we take the configuration sum for those tensor indices inside the cluster, leaving those on the border that become new tensor indices of the extended tensor. Because of the fractal geometry, some of the bonds inside the cluster are not connected with each other. We also take the configuration sum for these dangling bonds, and the process just changes the normalization of the partition function by an amount of

$$\sum_s W_{\sigma s} = 2\cosh\overline{K}[2(\cosh 2\overline{K})^{1/2}]^{-1/2} \tag{15}$$

for each, if we choose the definition of $W_{\sigma s}$ in Eq. (7). We take the rescaling effect into account, although the rescaling is not essential to the thermodynamic properties of the system, in particular, to its critical singularity. In this manner, what we are dealing with is the Ising model, where there are only spins denoted by the open dots in Fig. 1.

At first, we have only four spins s, s', s'', and s''' on the outgoing bonds, and after n extensions of the system, we have 4×2^n border spins on the *surface* of the extended cluster. The application of the HOTRG to this fractal system is straightforward. The recursive structure of the lattice is suitable for the repeated process of system extensions and renormalization group transformations in the HOTRG method. The partition function $Z_n(T)$ of the system after n extensions is obtained by a contraction of the extended tensors; we choose the periodic boundary conditions to evaluate

$$Z_n(T) = \sum_{ij} T^{(n)}_{ijij}, \tag{16}$$

where $T^{(n)}_{ijkl}$ is the renormalized local tensor obtained after n extensions.

III. NUMERICAL RESULTS

In order to simplify the numerical analysis, we choose the parametrization $J = k_B = 1$, and thus we have $K = 1/T$. In the numerical calculation by means of HOTRG, we keep $D = 24$ states at most for block spin variables. We have verified that the choice $D = 24$ is sufficient for obtaining the converged free energy

$$F_n(T) = -k_B T \ln Z_n(T) \tag{17}$$

in the entire temperature region [22]. We treat the free energy per site

$$f(T) = \lim_{n\to\infty} \frac{F_n(T)}{N_n} \tag{18}$$

in the following thermodynamic analyses, where the rhs converges already for $n \lesssim 30$.

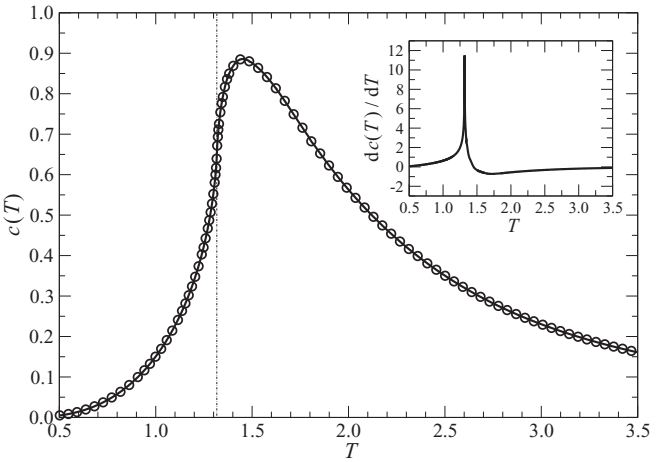

FIG. 2. The specific heat $c(T)$ per site in Eq. (19). Inset: Numerical derivative of $c(T)$ with respect to temperature; a sharp peak is observed at $T_c \approx 1.317$.

Figure 2 shows the temperature dependence of the specific heat per site

$$c(T) = \frac{\partial}{\partial T} u(T), \tag{19}$$

where $u(T)$ is the internal energy per site

$$u(T) = -T^2 \frac{\partial}{\partial T}\frac{f(T)}{T}, \tag{20}$$

and the temperature derivatives are performed numerically. There is no singularity in $c(T)$ around its maximum. One might find a weak nonanalytic behavior at $T_c \approx 1.317$, which is marked by the dotted line in the figure; the numerical derivative of $c(T)$ with respect to temperature (plotted in the inset) has a sharp peak at the critical temperature T_c. It is, however, difficult to determine the critical exponent α precisely, because of the weakness in the singularity; as shown in the figure, $c(T)$ around T_c is almost linear in T, and therefore α is nearly zero.

Figure 3 shows the spontaneous magnetization per site $m(T)$, which is obtained by inserting a σ-dependent local

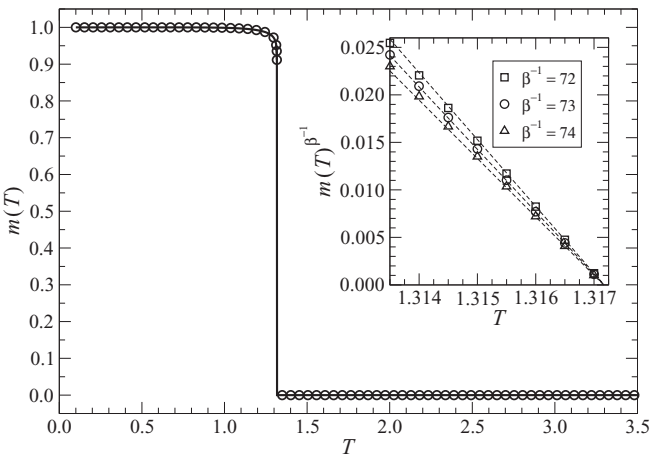

FIG. 3. The spontaneous magnetization per site $m(T)$. Inset: The power-law behavior below $T_c = 1.31716$.

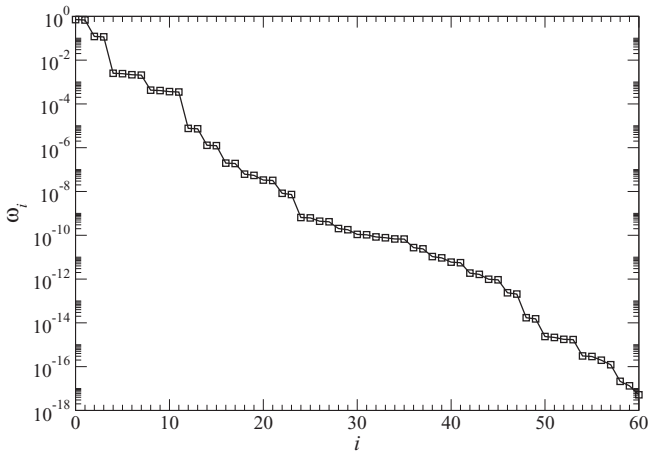

FIG. 4. Decay of the singular values after $n = 8$ extensions.

weight

$$\tilde{T}_{s\,s's''s'''} = \sum_{\sigma} \sigma\, W_{\sigma s}\, W_{\sigma s'}\, W_{\sigma s''}\, W_{\sigma s'''} \tag{21}$$

into the system. Since the fractal lattice is inhomogeneous, the value is weakly dependent on the location of the observation site, but the critical behavior is not affected by the location; we choose a site from the four sites that are in the middle of the 12-site cluster shown in Fig. 1. The numerical calculation by HOTRG captures the spontaneous magnetization $m(T)$ below T_c since any tiny round-off error is sufficient for breaking the symmetry inside the low-temperature ordered state. Around the transition temperature, the magnetization satisfies a power-law behavior

$$m(T) \propto |T_c - T|^{0.0137}, \tag{22}$$

where the precision of the exponent is around 2%, which can be read out from the inset of Fig. 3 as a tiny deviation from the linear dependence (the dashed lines) in $m(T)^{1/\beta}$ near T_c.

As a byproduct of the numerical HOTRG calculation, we can roughly observe the entanglement spectrum [23], which is the distribution of the eigenvalue ω_i of the density matrix that is created for the purpose of obtaining the block spin transformation. Since the effect of *environment* is not considered in our implementation of the HOTRG method, the eigenvalue $\omega_i = \lambda_i^2$ is obtained as the square of the singular values λ_i in the higher-order singular value decomposition applied to the extended tensors. Figure 4 shows ω_i at $T = T_c$ in decreasing order. The decay is rapid, and therefore a further increase of the number of block-spin states from $D = 24$ to a larger number does not significantly improve the precision in Z_n; the difference in $f(T_c)$ between $D = 8$ and $D = 16$ is already of the order of 10^{-6}. It should be noted that the eigenvalues are not distributed equidistantly in a logarithmic scale; the corner double line structure is absent [24,25].

IV. CONCLUSIONS AND DISCUSSIONS

We have investigated the Ising model on the fractal lattice shown in Fig. 1 by means of the HOTRG method. The calculated specific heat $c(T)$ suggests that the model shows a second-order phase transition. Qualitatively speaking, the presence of weak singularity in the specific heat agrees with the result of the ϵ expansion, which shows the increasing nature of the critical exponent in $c(T)$ with respect to the space dimension d [6]. The calculated spontaneous magnetization $m(T)$ also supports the second-order phase transition with the exponent $\beta_{\text{fractal}} \approx 0.0137$, which is smaller by one order of magnitude than the critical exponent $\beta_{\text{square}} = 1/8 = 0.125$ of the square-lattice Ising model.

The fractal structure of the lattice modifies the entanglement spectrum from that on the square lattice explained by the corner double line picture [24,25]. Since each corner is missing in the fractal structure in Fig. 1, short-range entanglement is almost filtered out in the process of the renormalization group transformation. This may be the reason why we do not need many degrees of freedom for the renormalized tensors. The situation is similar to the entanglement structure reported in the tensor network renormalization [26–31].

The lattice geometry of the fractal lattice can be modified in several ways. For example, one can alternate the system extension process of the fractal for the purpose of modifying the Hausdorff dimension; for every odd n, the extension with 12 vertices shown in Fig. 1 is performed, and for even n, the normal extension with 16 vertices on the square lattice is performed. Alternatively, one can also modify the basic cluster, in such a manner as introducing a 6×6 cluster where four corners are missing, etc. It is also worth considering a three-dimensional fractal lattice, and applying the HOTRG method as it was done for the cubic-lattice Ising model [19]. These modifications do not spoil the applicability of the HOTRG method while the numerical requirement is heavier than the current research. An analysis of quantum systems on a variety of fractal lattices is another possible extension [32,33]. These further studies may clarify the role of entanglement in the universality of the phase transition in both regular and fractal lattices.

ACKNOWLEDGMENTS

This work was supported by the projects VEGA-2/0130/15 and QIMABOS APVV-0808-12. T.N. and A.G. acknowledge support from a JSPS KAKENHI Grant No. 25400401.

[1] *Phase Transitions and Critical Phenomena*, edited C. Domb, M. S. Green, and J. Lebowitz (Academic, New York, 1972–2001), Vols. 1–20.

[2] H. E. Stanley, *Introduction to Phase Transitions and Critical Phenomena* (Oxford University Press, Oxford, UK, 1971).

[3] M. E. Fisher, Rev. Mod. Phys. **46**, 597 (1974), and references therein.

[4] L. P. Kadanoff, Physics **2**, 263 (1966).

[5] E. Efrati, Z. Wang, A. Kolan, and L. P. Kadanoff, Rev. Mod. Phys. **86**, 647 (2014).

[6] K. G. Wilson and J. Kogut, Phys. Rep. **12**, 75 (1974).
[7] J. Zinn-Justin, *Quantum Field Theory and Critical Phenomena* (Oxford University Press, Oxford, UK, 1996).
[8] Y. Gefen, B. B. Mandelbrot, and A. Aharony, Phys. Rev. Lett. **45**, 855 (1980).
[9] Y. Gefen, Y. Meir, B. B. Mandelbrot, and A. Aharony, Phys. Rev. Lett. **50**, 145 (1983).
[10] Y. Gefen, A. Aharony, and B. B. Mandelbrot, J. Phys. A **16**, 1267 (1983).
[11] Y. Gefen, A. Aharony, and B. B. Mandelbrot, J. Phys. A **17**, 1277 (1984).
[12] Y. Gefen, A. Aharony, Y. Shapir, and B. B. Mandelbrot, J. Phys. A **17**, 435 (1984).
[13] J. H. Luscombe and R. C. Desai, Phys. Rev. B **32**, 1614 (1985).
[14] T. Stošić, B. D. Stošić, S. Milošević, and H. E. Stanley, Physica A **233**, 31 (1996).
[15] M. Wang, S. J. Ran, T. Liu, Y. Zhao, Q.-R. Zheng, and G. Su, arXiv:1311.1502 (to be published).
[16] A. Vezzani, J. Phys. A **36**, 1593 (2003).
[17] J. M. Carmona, U. Marini, B. Marconi, J. J. Ruiz-Lorenzo, and A. Tarancon, Phys. Rev. B **58**, 14387 (1998).
[18] *Real-Space Renormalization*, edited by T. W. Burkhardt and J. M. J. van Leeuwen, Topics in Current Physics Vol. 30 (Springer, Berlin, 1982), and references therein.
[19] Z. Y. Xie, J. Chen, M. P. Qin, J. W. Zhu, L. P. Yang, and T. Xiang, Phys. Rev. B **86**, 045139 (2012).
[20] M. E. Fisher, Proc. R. Soc. London, Ser. A **254**, 66 (1960).
[21] The symmetry in the local tensors is not always preserved when one performs the renormalization group transformation in the HOTRG method. Thus, for most of the cases, the symmetry is not that important in the numerical calculations.
[22] A larger value of D is necessary if one needs tiny density-matrix eigenvalues for the purpose of analyzing their asymptotic decay.
[23] It is possible to identify the system boundary of a finite area of two-dimensional classical lattice models as "a wave function" of a certain one-dimensional quantum system. In this manner, one naturally finds the quantum-classical correspondence, and can introduce the notion of entanglement in classical lattice models.
[24] Z. C. Gu and X. G. Wen, Phys. Rev. B **80**, 155131 (2009).
[25] H. Ueda, K. Okunishi, and T. Nishino, Phys. Rev. B **89**, 075116 (2014).
[26] G. Evenbly and G. Vidal, Phys. Rev. Lett. **115**, 180405 (2015).
[27] G. Evenbly and G. Vidal, Phys. Rev. Lett. **115**, 200401 (2015).
[28] G. Evenbly, arXiv:1509.07484.
[29] G. Evenbly and G. Vidal, arXiv:1510.00689.
[30] M. Hauru, G. Evenbly, W. W. Ho, D. Gaiotto, and G. Vidal, arXiv:1512.03846.
[31] S. Yang, Z. C. Gu, and X. G. Wen, arXiv:1512.04938.
[32] A. Voigt, J. Richter, and P. Tomczak, Physica A **299**, 461 (2001).
[33] A. Voigt, W. Wenzel, J. Richter, and P. Tomczak, Eur. Phys. J. B **38**, 49 (2004).